Asymmetric Shunt Inductance Iris Rectangular Waveguide Filters for Satellite Communication Systems

H*icham SETTI*[1]**, A. Maimouni,*[2]*A. Tribak*[3]*, and O. Souna*[1]

[1]FPL, Advanced Sciences and Technologies Lboratory,University of Abdelmalek Essaidi Larache Morocco,
[2] Physics Department College of Science, University of Imam Muhammad Bin Saud Islamic, Riyadh-Saudi Arabia
[3]INPT, Microwave Group, INPT Rabat Morocco

Abstract. This paper presents the design, simulation and manufacture of two Asymmetrical filters based respectively on standard rectangular waveguides WR90 and WR75 in which resonant irises are inserted, operating respectively in the X-Band [9-11GHz] and Ku-Band [11-13GHz].The filter parameters were simulated by the MMM modal matching method (MMM) implemented in the Microwave-Wizard software, and that obtained by the CST-MWS software. The simulated results are in good agreement with those obtained by the experimental measurements.

Keywords: Filters, Waveguide, iris, Asymmetric Shunt Inductance.

1 Introduction

The microwave frequency domain is widely used by telecommunications networks. Optimal use of the frequency spectrum requires very high channel selectivity, which has enabled an increasing number of users of the frequency spectrum. Filters are essential devices that are key elements in determining the performance of telecommunications systems; they represent a major and very important part in the field of modern fixed or mobile communications, land or space. This has created both very demanding performance specifications for filters and commercial pressures to reduce costs.

In the design of microwave or millimeter wave components, discontinuities play a particularly important role. These discontinuities are used to perform various types of functions: filtering, phase shifting, power matching, etc.

In the case of our evanescent mode filters, the discontinuities are created by obstacles made up of symmetrical or asymmetrical rectangular irises. Many methods have been used to model the uniaxial discontinuities in cascade [1] - [7], the dispersion matrix of the set will be obtained by carrying out the scattering of the individual discontinuities, assimilated to multi-poles and separated from each other by waveguide sections of lengths equal to the distances between the discontinuities.

We present the procedure for designing and producing iris filters. The modeling of the various discontinuities is analyzed by the modal Matching method (MMM). The scattering of the set will be obtained by chaining the generalized scattering (GSMs) of the individual discontinuities [8], [9] - [15].

We propose in this paper, two band-pass filters in waveguide technology having rectangular symmetrical discontinuities, designed and tested respectively in the band [9-11] GHz and the band [11-13] GHz. These filters consist of 8 irises placed asymmetrically respectively in a standard WR90 and WR 75 waveguide. These irises are used to very strongly couple the sections in this filter, which allows to increase the bandwidth and to control the matching.

2 Design of Asymmetrical Iris Filter

Rectangular waveguide microwave bandpass filters composed of coupling irises are used extensively in telecommunications systems today. Their main quality is to withstand very high powers by creating low insertion losses. The conventional procedure for producing this type of filter is based on the fundamental TE mode which resonates n times in the structure (n resonant cavities coupled by irises). The Ki+1 element simulate the coupling irises. These inverters cannot be produced using passive elements alone. Their implementation requires the use of elements with distributed constants of negative electrical length, which are absorbed by the adjacent resonant cavities. The coupling irises have purely inductive impedance. The equivalent electrical circuit must be equivalent to an impedance inverter [16].

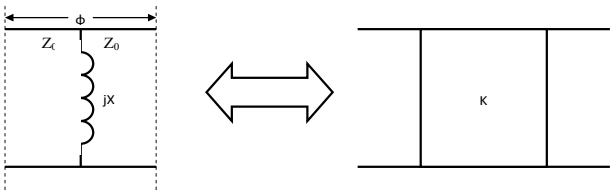

Fig 1. Electrical diagram equivalent to the impedance inverter

An iris is equivalent to a pure reactance and two sections of line of characteristic impedance Z0 and of total electrical length Φ.

* Corresponding author: hsetti1981@gmail.com

Taking into account the normalized susceptance $\hat{B} = 0$, the ABCD matrix is the product of the ABCD matrix of these three elements [18].

$$\begin{pmatrix} 0 & jK \\ \frac{j}{K} & 0 \end{pmatrix} = \begin{bmatrix} cos\left(\frac{\phi}{2}\right) - \frac{\hat{B}}{2}sin(\phi) & jZ_0\left[sin(\phi) - \hat{B}sin^2\left(\frac{\phi}{2}\right)\right] \\ jY_0\left[sin(\phi) - \hat{B}sin^2\left(\frac{\phi}{2}\right)\right] & cos\left(\frac{\phi}{2}\right) - \frac{\hat{B}}{2}sin(\phi) \end{bmatrix}$$

By comparing the equality of the two terms of the above equation, the equality is checked if:

$$\begin{cases} \phi = -arctan\ \frac{2}{\hat{B}} \\ \hat{B} = \frac{Z_0}{K} - \frac{K}{Z_0} \end{cases}$$

The expression for Φ shows that the electrical lengths introduced by the irises are negative and therefore absorbed by the lengths of the adjacent cavities.
The negative phase shift introduced by the irises Φi-1/2 and Φi + 1/2 is compensated by the electrical length θi; of the ith cavity of the filter. This is illustrated in the following figure [16]:

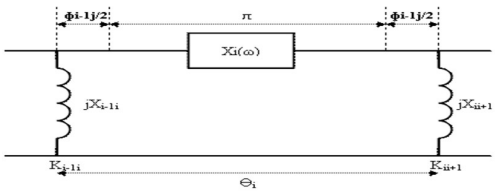

Fig 2. Resonant cavity surrounded by irises at its ends

Resonant cavities are half-wave lines; their electrical length is equal to:

$$\theta_i = \beta l = \frac{2\pi}{\lambda_g}\frac{\lambda_g}{2} = \pi$$

The electrical lengths θi are adjusted so that the electrical length between two consecutive inverters is equal to:

$$\theta_i = \pi + \frac{1}{2}\left[\phi_{i-1,i} + \phi_{i,i+1}\right]$$

This corresponds to:

$$\theta_i = \pi - \frac{1}{2}\left[\arctan\frac{2X_{i-1,i}}{Z_0} + \arctan\frac{2X_{i,i+1}}{Z_0}\right]$$

The physical length of the cavities depends on the electrical length and the wavelength in the guide.

$$l_i = \frac{\lambda_{g_0}}{2}\frac{\theta_i}{\pi}$$

In other words :

$$l_i = \frac{\lambda_{g_0}}{2} - \frac{\lambda_{g_0}}{4}\left[\arctan 2\frac{X_{i-1,i}}{R_0} + \arctan 2\frac{X_{i,i+1}}{R_0}\right] \quad (*)$$

When designing waveguide filters with discontinuities, one will need to use many analytical models modeling these discontinuities. For the sizing of these discontinuities, approximation equations valid for zero iris width have been given in this article to determine the dimensions of asymmetric irises. The passage from the localized bandpass filter to the volume filter and the analytical iris models will be used during the synthesis of the inductive iris bandpass filters. The negative component introduced by the irises is negligible compared to the length of the resonant cavity.

For the current design, E plane Asymmetrical iris structure is preferred as shunt inductors which is also known as H plane waveguide filter [17]. This structure is named as shunt inductance asymmetrical iris and the most accurate one in terms of bandwidth, return loss and center frequency responses and also it is easy to implement [18]. Thus, it is mostly chosen in waveguide filter applications.

l_i is the distance between two consecutive irises waveguide cavity, can be found using the formula given in Eq. (∗) [18].

$$l_i = \frac{\lambda_{g0}}{2\pi}\left(\pi + \frac{\emptyset_i}{2} + \frac{\emptyset_{i+2}}{2}\right)$$

$\frac{\emptyset_i}{2}$ and $\frac{\emptyset_{i+2}}{2}$ seen in Eq. (*) are the electrical lengths of transmission line sections with negative lengths at two sides of shunt inductances shown in Figure 2. The total electrical lengths between two consecutive irises are $\pi + \frac{\emptyset_i}{2} + \frac{\emptyset_{i+2}}{2}$.

The geometry of shunt inductor asymmetrical iris structure is given in Figure 3. In the case of an asymmetric inductive iris, a single metal plate is inserted on one side of the waveguide. The equivalent electrical diagram and the geometry of this obstacle which produces an inductive effect are shown in figure 3.

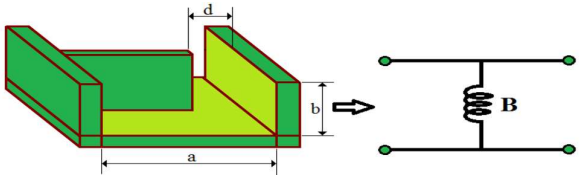

Fig 3. Asymmetric inductive iris

The relation between the normalized susceptance $\hat{B}$ and the distance d shown in the figure above is given by [16]:

$$\hat{B} = \frac{2\pi}{\beta a}\cot^2\left(\frac{\pi d}{2a}\right)\left[1 + \csc^2\left(\frac{\pi d}{2a}\right)\right]$$

The topology of the asymmetric inductive iris bandpass filter is shown in figure 4. The inductive irises appear as non-symmetrical openings at the ends of the guide cavities after each half wavelength λ / 2.

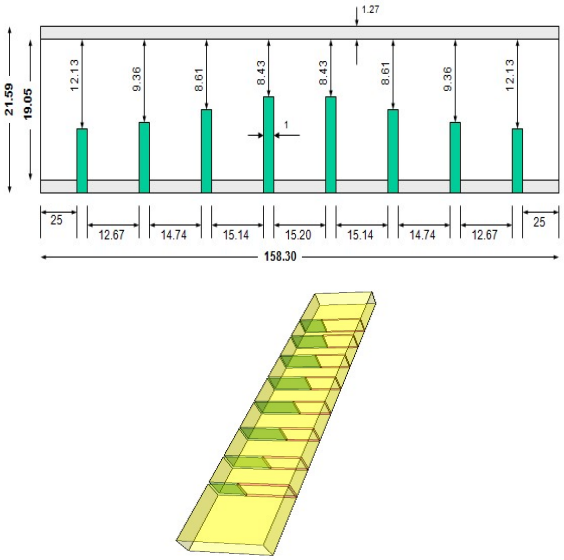

Fig 4: Geometric structure of the asymmetric inductive iris filter

3 Simulation and Experimental Results

In the two prototypes we tested, we used 8 iris discontinuities separated by quarter-wavelength cavities. Figure 5 shows a mechanical prototype of one of the two symmetrical filters.

Fig 5: Prototype of a symmetrical filter formed by 8 symmetrical iris discontinuities.

The two filters that we have analyzed are asymmetrical and consist respectively of rectangular waveguides WR90 and WR75 in which resonant irises are inserted. Figure 6 and figure 7 show the comparison between theoretical and experimental results.

From the previous figures comparing the theoretical and experimental results of the parameters of the diffraction matrix S11 and S21, it can be seen very clearly, on these curves, that the measurements give results almost similar to the theoretical results over the entire frequency range of interest; the slight increase in the reflection coefficient in the passband is due to the problem of miniaturization during the mechanical manufacture of filters. In the modal adaptation method that we used to characterize the four filters, we used a number of modes N between 30 and 60.

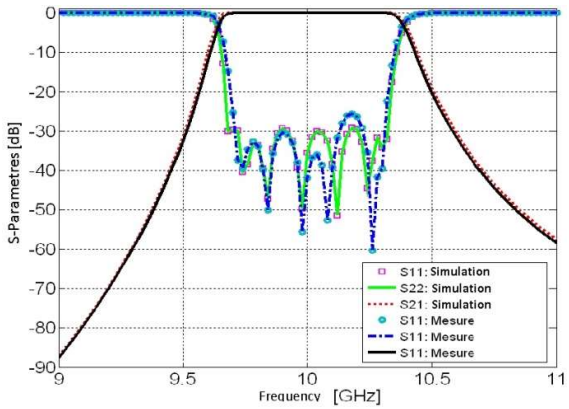

Fig 6: Comparison of theoretical reflection coefficients and those obtained by measurements, X band (WR90).

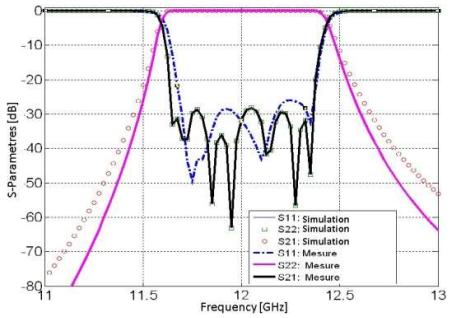

Fig 7: Comparison of theoretical reflection coefficients and those obtained by measurements, Ku band (WR75).

As we can observe in both cases, we obtained a good agreement between the theoretical and experimental results.
We notice that the results obtained using the two tools simulation is in agreement with those resulting from the experimental results. We note a good consistency between the results. This also demonstrates the ability of Mician and CST to design this type of filter. The bandwidth of this filter is on the order of 1 GHz and its center frequency is close to 9.9 and 12.18 GHz respectively. We notice a good matching characterized by a reflection coefficient around (-30 dB), and insertion loss around (-0.05 dB) in the band of interest.

Table1: Comparison of this work with others

Ref	F_c (GHz)	IL (dB)	RL (dB)
This work	9.9 and 12.2	0.05	30
[19]	14.25	0.35	30
[20]	10	1.4	25
[21]	3.6	3.7	12

IL: Insertion loss over the whole pass-band.
RL: Return loss over the whole pass-band.
F_c: The central frequency.

To further demonstrate the performance of these filters, table 1 is provided for comparison of this work with other works which are all based on wide band pass filter category. A comparison of the main performances of waveguide filters is listed.

4 Conclusion

In summary, we have presented two asymmetrical filters based respectively on standard rectangular waveguides WR90 and WR75 in which resonant irises are inserted, operating respectively in the X-Band [9-11GHz] and Ku-Band [11-13GHz]. The simulated results are in good agreement with those obtained by the experimental tests. The bandwidth of this filter is on the order of 1 GHz and its center frequency is close to 12.18 and 9.9 GHz respectively. We notice a good ports matching characterized by a reflection coefficient around (-30 dB) in two bands.

5 References

1. G.Matthaei,L.Young,Gand.M.T.Jones, "Microwave filters, impedance-matching networks, And coupling structures",pp.320-334,McGraw-Hill,new York,1964.
2. P. A. Rizzi "Microwave engineering passive circuits ", pp.306-317 pp 454-489, Prentice-Hall, Inc.1988.
3. A. Mediavilla, A. Tazon, J.A. Pereda, M. Lazaro, I. Santamaria, C. Pantaleon, "Neuronal Architecture for Waveguide Inductive Iris Bandpass Filter Optimization," ijcnn, p. 4395, IEEE-INNS-ENNS International Joint Conference on Neural Networks (IJCNN'00)-Volume 4, 2000.
4. Teberio, F., Arregui, I., Guglielmi, M., Gomez-Torrent, A., Soto, P., Laso, M. A. G., & Boria, V. E. (2016). Compact broadband waveguide diplexer for satellite applications. IEEE MTT-S International Microwave Symposium Digest, 2016-Augus(1), 2–5. https://doi.org/10.1109/MWSYM.2016.7540231
5. D. L. BOYENGA, « Contribution à la nouvelle formulation variationnelle : Application aux études des discontinuités et des filtres en guides d'ondes métalliques", thèse de doctorat INP Toulouse, Nov. 2005.
6. Nosrati, M., & Daneshmand, M. (2018). Gap-Coupled Excitation for Evanescent-Mode Substrate Integrated Waveguide Filters. IEEE Transactions on Microwave Theory and Techniques, 66(6). https://doi.org/10.1109/TMTT.2018.2818155
7. Mohottige, N., Budimir, D., Golubicić, Z., & Potrebic, M. (2011). Electromagnetic modelling of dielectric-filled waveguide filters for diplexer applications. IEEE Antennas and Propagation Society, AP-S International Symposium (Digest), 873–875. https://doi.org/10.1109/APS.2011.5996414
8. J. Uher, J. Bohrnemann, and U. Rosenberg, Waveguide components for antenna feed systems: Theory and CAD, Chapter 3, Boston, Artech. House, 1993.
9. Mohammadi, E., & Ghorbaninejad, H. (2017). Novel resonant structure to compact partial H-plane band-pass waveguide filter. International Journal of Electrical and Computer Engineering, 7(1), 266–270. https://doi.org/10.11591/ijece.v7i1.pp266-270
10. R. Levy, "Derivation of equivalent circuits of microwave structures using numerical techniques," IEEE Trans. Microw. Theory Tech., vol. 47, pp. 1688. 1695, Sept. 1999.
11. Li, P., Chu, H., & Chen, R. S. (2017). Design of compact bandpass filters using quarter-mode and eighth-mode SIW cavities. IEEE Transactions on Components, Packaging and Manufacturing Technology, 7(6). https://doi.org/10.1109/TCPMT.2017.2677958

12. J.Bornemann, "Comparison between different formulations of the transverse resonance field-matching technique for the three-dimensional analysis of metal finned waveguide resonators," in J. Numerical Modeling., vol.4, pp.63-73, March 1991.
13. Fu, Y., Yang, B., & Miao, J. (2013). Exact Design of A Ka Band H-plane Inductance Diaphragm Waveguide Band-pass Filter. 1618–1621. https://doi.org/10.1109/GreenCom-iThings-CPSCom.2013.293
14. "V. E. Boria and B. Gimeno, 'Waveguide filters for satellite', IEEE Microwave Magazine, vol. 8, pp. 60-70, Oct. 2007.
15. Chu, H., Li, P., & Chen, J. X. (2015). Balanced substrate integrated waveguide bandpass filter with high selectivity and common-mode suppression. IET Microwaves, Antennas and Propagation, 9(2). https://doi.org/10.1049/iet-map.2013.0708
16. (G. Bianchi. Electronic Filter Simulation & Design . McGraw-Hill Professional, 1 edition, 2007, n.d.)*
17. L. Li, Z. Wu, K. Yang, X. Lai, and Z. Lei, "A Novel Miniature Single-Layer Eighth-Mode SIW Filter with Improved Out-of-Band Rejection," IEEE Microw. Wirel. Components Lett., vol. 28, no. 5, pp. 407–409, 2018.
18. "R. Levy, R.-V. Snyder, and G. Matthaei,"Design of microwave filters", IEEE Trans. Microwave Theory and Thech., vol. 50, no.3 , pp. 783-793, Mar.2002."
19. Pons-Abenza, A., García-Barceló, J. M., Romera-Pérez, A., Alvarez-Melcon, A., Quesada-Pereira, F. D., Hinojosa-Jiménez, J., Guglielmi, M., Boria Esbert, V. E., & Arche-Andradas, L. (2020). Design and implementation of evanescent mode waveguide filters using dielectrics and additive manufacturing techniques. AEU - International Journal of Electronics and Communications, 116(X), 1–9.https://doi.org/10.1016/j.aeue.2020.153065
20. Vallerotonda, P., Pelliccia, L., Tomassoni, C., Cacciamani, F., Sorrentino, R., Galdeano, J., & Ernst, C. (2019). Compact waveguide bandpass filters for broadband space applications in c and ku-bands. Proceedings of European Microwave Conference in Central Europe, EuMCE 2019, May, 116–119.
21. Zou, X., Tong, C. M., & Yu, D. W. (2011). Design of an X-band symmetrical window bandpass filter based on substrate integrated waveguide. Proceedings of 2011 Cross Strait Quad-Regional Radio Science and Wireless Technology Conference, CSQRWC 2011, 1, 571–574. https://doi.org/10.1109/CSQRWC.2011.6037014